Expansion and Contraction of the Sahara Desert from 1980 to 1990

COMPTON J. TUCKER, HAROLD E. DREGNE, WILBUR W. NEWCOMB

Data from polar-orbiting meteorological satellites have been used to determine the extent of the Sahara Desert and to document its interannual variation from 1980 to 1990. The Sahara Desert ranged from 8,633,000 square kilometers in 1980 to 9,982,000 square kilometers in 1984. The greatest annual north-south latitudinal movement of the southern Saharan boundary was 110 kilometers from 1984 to 1985 and resulted in a decrease in desert area of 724,000 square kilometers.

THE LARGEST DESERT OF OUR PLANet, the Sahara of Africa, is between ~7,000,000 and ~9,000,000 km^2 in area. The northern boundary has been arbitrarily set to follow the south side of the Atlas Mountains to Biskra (Algeria) where it dips southward through Tunisia to the Gulf of Gabes and from there continues along the Mediterranean to the Suez Canal (*1*). The southern boundary stretches east to west at ~16° to 17°N for 6000 km from the Atlantic Ocean in Mauritania to the Red Sea in Sudan and is a vegetation-zone boundary. At this boundary there is an almost insensible gradient of plants, animals, and physiographic characteristics into steppe vegetation of the Sahel zone (*2, 3*) resulting from a mean annual precipitation gradient of ~1 mm year^{-1} km^{-1} from north to south. Uncertainty in and variation of the location of the boundary between the Sahara and the Sahel zone has prevented precise estimates of the extent of the Sahara (*4*).

Although deserts share a number of features (climate, weather, and a low density of vegetation), most workers have defined "desert" according to their discipline (*5, 6*). We use "desert" to be synonymous with "arid." "Semiarid" represents the gradation of desert into "steppe" and denotes areas of less aridity, higher and more evenly distributed rainfall, and higher levels of primary production. "Steppe" is also imprecise, and its use varies widely (*6*).

Largely anecdotal information suggests that the Sahara has expanded toward the south (*7–12*). The alleged expansion was attributed in part to climate variation (droughts) (*13*) and to land mismanagement such as overgrazing, increased cultivation, and firewood cutting (*8, 11*). This process of land degradation is called "desertification" by some (*14*) and "desertization" by others (*15*). The occurrence of a period of wet years (1950 to 1968) followed by dry years (1969 to 1990) has also contributed to the controversy over the location of the southern Sahara boundary (Fig. 1) (*16–18*).

Lamprey (*12*) compared the location of the southern boundary of desert vegetation in western Sudan in 1958 with its location in 1975. He estimated that the boundary had shifted southward by 90 to 100 km during the 17-year period, a desert expansion of ~5.5 km year^{-1}; this value has been repeated often in the popular press (*9–11*). However, a 1984 field study by Hellden (*19*) in the same area found no evidence of such an expansion.

In order to measure directly the changes in vegetation at this boundary, we used a satellite-derived vegetation index to map interannual changes in vegetative cover and, by inference, rainfall, along the Saharan-Sahelian boundary from the Atlantic Ocean to the Red Sea for the period 1980 to 1990. We hypothesized that annual variations in rainfall would bring corresponding changes in the density of vegetative cover. Malo and Nicholson (*20*) have shown that the satellite-derived vegetation index we used is linearly related to precipitation in the area of our study (Fig. 2).

Vegetation indices are spectral measures derived from remotely sensed data in the red and near-infrared spectral regions. The red spectral response is inversely related to the chlorophyll density, and the near-infrared spectral response is directly related to scattering in individual leaves and between leaves in the canopy. Combining data from these two adjacent spectral regions compensates for differences in irradiance and provides an estimate of the intercepted fraction of the photosynthetically active radiation or photosynthetic capacity (*21*). These data are also strongly related to total primary production when summed or averaged over the growing season (*22*). We used a satellite-derived vegetation index calculated from meteorological satellite data and expressed this index in terms of estimated annual precipitation (Fig. 2).

The area we studied lies between 16°W and 39°E longitude and 10° and 25°N latitude. This area includes a sizable part of the Sahara Desert as well as the Sahel (*23–25*). We will use the 200 mm year^{-1} precipitation isoline as the boundary between the Sahara Desert and the Sahel zone, realizing that this is actually the boundary between the Sahel proper and the Saharan-Sahelian transition zone. This is unavoidable as the utility of our satellite vegetation index approach is limited below the ~150 to 200 mm year^{-1} precipitation isoline because of limited green vegetation.

Satellite data from the U.S. National Oce-

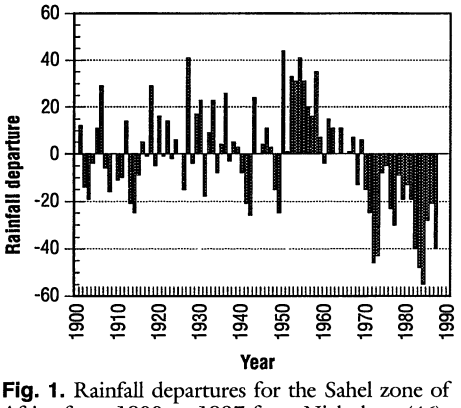

Fig. 1. Rainfall departures for the Sahel zone of Africa from 1900 to 1987 from Nicholson (*16*). Note the period of wet years and dry years, especially from 1950 through the present.

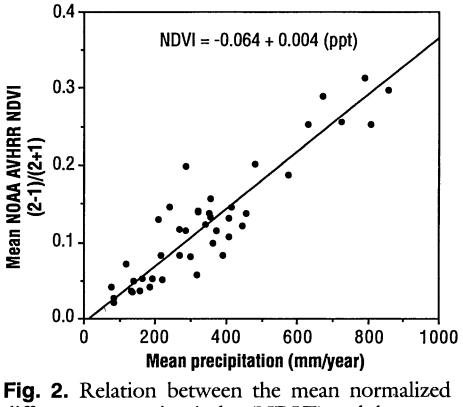

Fig. 2. Relation between the mean normalized difference vegetation index (NDVI) and the mean annual precipitation for 1982 to 1985; ppt, parts per thousand.

C. J. Tucker and W. W. Newcomb, Laboratory for Terrestrial Physics, National Aeronautics and Space Administration Goddard Space Flight Center, Greenbelt, MD 20771.
H. E. Dregne, International Center for Arid and Semi-Arid Land Studies, Texas Tech University, Lubbock, TX 79409.

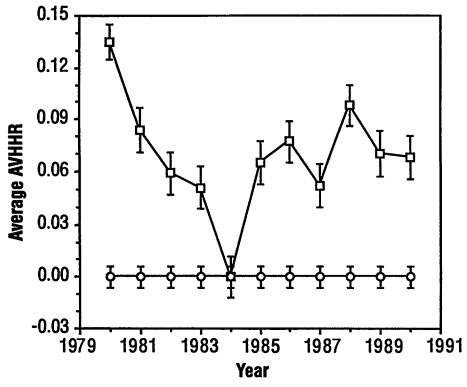

Fig. 3. Average vegetation index values for the approximate 200 to 400 mm year^{-1} long-term mean precipitation zone (□) and the Sahara Desert (○) from 1980 to 1990; 1984 was an exceptionally dry year (see also Fig. 1). There is a direct relation between primary production and the vegetation index (*22*), precipitation and primary production (*28*), and hence precipitation and the vegetation index (Fig. 2).

anic and Atmospheric Administration's (NOAA) polar-orbiting meteorological satellites were used from 1980 to 1990. Data from the advanced very high resolution radiometer (AVHRR) channel 1 (0.55 to 0.68 μm), channel 2 (0.73 to 1.1 μm), and channel 5 (11.5 to 12.5 μm) were used to calculate the normalized difference vegetation index (NDVI) (*26*).

The NDVI was computed for the Sahel zone as well as for a 1,000,000 km^2 area of the central Sahara and plotted against year (Fig. 3). Rainfall and hence primary production decreased progressively from 1980 to 1984 in the Sahel zone (Figs. 1 and 3). Nicholson has reported that 1980 had a rainfall departure of about −13% from the long-term mean precipitation for the Sahel zone, and 1984 was one of the driest years this century (*16, 17*). Higher mean values for the NDVI for the Sahel zone were found for 1985 to 1990 than for 1984; these values indicate that conditions improved in 1985 to 1990 as compared to 1984. Significant variation in the NDVI was observed in the Sahel zone over the 11 years of observation; 1980 was the year of the highest NDVI and 1984 the lowest. This observation is in agreement with the meteorological data of Nicholson (*16*) and Lamb *et al.* (*17*). Annual precipitation for all 11 years of our study was below the long-term mean.

Our data document a progressively southward movement of the Saharan-Sahelian boundary (the 200 mm year^{-1} precipitation isoline) from 1980 to 1984 of 240 km (~60 km year^{-1}). We computed this rate by averaging the boundary location at each half degree of longitude from 15.5°W to 38.5°E (Table 1). We estimate that the error associated with our boundary determination is ±2 pixels or 15 km.

The average southward movement of the Saharan-Sahelian boundary (the 200 mm year^{-1} annual precipitation isoline) from 1980 to 1981 was 55 km, from 1981 to 1982 was 77 km, from 1982 to 1983 was 11 km, and from 1983 to 1984 was 99 km. From 1984 to 1985 there was south-to-north movement (retreat of the desert) of 110 km followed by a further northward movement from 1985 to 1986 of 33 km. In 1987 the mean position moved

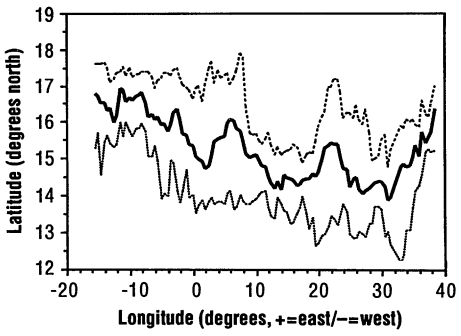

Fig. 4. Summary of the mean (dark line), most northern (dashed line), and most southern (light line) position of the 200 mm year^{-1} boundary location from 1980 to 1990 at every 0.5° of longitude from 15.5°W to 38.5°E. We estimate the error to be ±15 km (±0.14°). See also Table 1.

southward 55 km. In 1988, it moved northward 100 km; in 1989 and 1990 it again moved southward 44 and 33 km, respectively. The mean position in 1990 was thus ~130 km south of its position in 1980. Desert expansion varied in the 11 years of our analysis from 248,000 km^2 (1988) to 1,349,000 km^2 (1984), all relative to 1980. The 1984 expansion represents a 15% increase in the size of the Sahara as compared with 1980. We estimated that the area of the Sahara and the Sahara-Sahelian transition zone was 8,633,000 km^2 in 1980 (Table 1).

The north-south movement of the 200 mm year^{-1} isoline varied greatly across the south side of the Sahara (Fig. 4). Variation was high from Mali through central Niger and from eastern Chad through western Sudan. Variation was low in southern central and southeastern Mauritania and from central Niger through western Chad. Rainfall, and hence vegetation distributions, vary in space as well as in time in this area.

The observed low variability in the interannual movement of the 200 mm year^{-1} isoline in Mauritania and from central Niger through western Chad has implications for detecting desertification. The ability to detect changes should increase in areas of lower interannual variability. Interannual variations mean that it would require a decades-long study to determine whether long-term expansion or contraction of the Sahara is occurring. Our data provide a baseline for comparison with future data (*27*).

Table 1. Area of the Sahara Desert and the Saharan-Sahelian transition zone from 1980 to 1990 with the estimated 200 mm year^{-1} precipitation isoline as the southern boundary. In the central Sahara, the Adrar des Iforas, Air, and Tibesti mountain areas were included as were the desert areas for the Eastern Desert of Egypt and the Nubian Desert of Sudan. Changes are relative to 1980. Nicholson's (*16*) Sahelian mean annual precipitation departures from the long-term mean are given from 1980 to 1987. The northern boundary of the Sahara was the line running from Wadi Draa (29°N, 10.5°W) on the Atlantic coast along the Saharan Fault to Figuig (32°N, 2°W), Morocco, from there to Biskra (35°N, 6°E), Algeria, and from there southward through Tunisia to the Gulf of Gabes (34°N, 10°E). Areas of cultivation on the Mediterranean coast were excluded as was the Nile delta and river valley. We estimate the mean latitude position error to be ±15 km. The error associated with the total Saharan area is estimated to be ±90,000 km^2 and is the product of the north-south error (±15 km or ±0.14° of latitude) and the length of the southern boundary (6000 km). The standard deviation appears in parentheses. ND, no data.

Year	Saharan area (km^2)	Change relative to 1980 (km^2)	Annual precipitation departure (%) (*16*)	Mean latitude and range of the 200 mm year^{-1} isoline (deg)
1980	8,633,000	0	−13	16.3 (0.9) 14.3 to 17.9
1981	8,942,000	308,000	−19	15.8 (1.1) 14.1 to 17.6
1982	9,260,000	627,000	−40	15.1 (0.9) 12.9 to 16.7
1983	9,422,000	789,000	−48	15.0 (0.9) 13.3 to 16.7
1984	9,982,000	1,349,000	−55	14.1 (1.0) 12.1 to 17.0
1985	9,258,000	625,000	−28	15.1 (0.9) 13.3 to 17.3
1986	9,093,000	460,000	−21	15.4 (0.8) 14.0 to 17.1
1987	9,411,000	778,000	−40	14.9 (0.9) 13.3 to 16.8
1988	8,882,000	248,000	ND	15.8 (0.8) 14.2 to 17.3
1989	9,134,000	501,000	ND	15.4 (1.3) 12.8 to 17.6
1990	9,269,000	635,000	ND	15.1 (1.1) 12.8 to 17.4

REFERENCES AND NOTES

1. W. G. McGinnies, B. J. Goldman, P. Paylore, *Deserts of the World* (Univ. of Arizona Press, Tucson, 1968); J. L. Cloudsley-Thompson, *Sahara Desert* (Pergamon, New York, 1984); J. Swift, *The Sahara* (Time-Life Books, New York, 1975).
2. H. N. Le Houerou, *J. Range Manage.* **33**, 41 (1980).
3. T. Monod, in *Ecosystems of the World: Hot Deserts and Arid Shrublands*, M. Evenari, I. Noy-Meir, D. W. Good-

all, Eds. (Elsevier, New York, 1985), pp. 203–243.
4. We include the Nubian Desert of Sudan, the Eastern and Western deserts of Egypt, the Libyan Desert, and all other subdeserts of North Africa contiguous to the Sahara in our figures for the Sahara.
5. D. W. Goodall and R. A. Perry, Eds., *Arid-Land Ecosystems: Structure, Functioning, and Management* (Cambridge Univ. Press, Cambridge, 1979), vol. 1; W. G. McGinnies, *ibid.*, pp. 299–314; A. Shmida, in *Ecosystems of the World: Hot Deserts and Arid Shrublands*, M. Evenari, I. Noy-Meir, D. W. Goodall, Eds. (Elsevier, New York, 1985), pp. 23–77.
6. M. Evenari, in *Ecosystems of the World: Hot Deserts and Arid Shrublands*, M. Evenari, I. Noy-Meir, D. W. Goodall, Eds. (Elsevier, New York, 1985), pp. 1–22.
7. F. R. Cana, *Geogr. J.* **46**, 333 (1915); E. W. Bovill, *J. Afr. Soc.* **20**, 175 (1921); *ibid.*, p. 259; E. P. Stebbing, *Geogr. J.* **85**, 506 (1935); F. Rodd, *ibid.* **91**, 354 (1938); E. P. Stebbing, *ibid.*, p. 356; A. Aubreville *et al.*, *Bois For. Trop.* **148**, 3 (1973).
8. E. Eckholm and L. R. Brown, *Worldwatch Paper 13* (Worldwatch Institute, Washington, DC, 1977), p. 1.
9. J. Smolowe, *Time* **127** (no. 33), 36 (1987).
10. C. Norman, *Science* **235**, 963 (1987).
11. W. S. Ellis, *Natl. Geogr.* **172**, 140 (1987).
12. H. F. Lamprey, "Report on the desert encroachment reconnaissance in Northern Sudan" (Unesco/UNEP) [*Desertification Control Bull.* **17**, 1 (1988)].
13. S. E. Smith, *J. Soil Water Conserv.* **41**, 297 (1986).
14. M. Kassas, in *Arid Lands in Transition*, H. E. Dregne, Ed. (AAAS, Washington, DC, 1970), pp. 123–142.
15. H. N. Le Houerou, *Ann. Alger. Geogr.* **6**, 2 (1968).
16. S. E. Nicholson, *Weather* **44**, 47 (1989).
17. P. J. Lamb, R. A. Peppler, S. Hastenrath, *Nature* **322**, 238 (1986).
18. C. Toupet, *C. R. Somm. Seances Soc. Biogeogr.* **48**, 39 (1972).
19. U. Hellden, *Drought Impact Monitoring* (Lund University Naturgeografiska Institute, Lund, Sweden, 1984).
20. A. R. Malo and S. N. Nicholson, *J. Arid Environ.* **19**, 24 (1990).
21. P. J. Curran, *Philos. Trans. R. Soc. London Ser. A* **309**, 257 (1983); C. J. Tucker and P. J. Sellers, *Int. J. Remote Sensing* **7**, 1395 (1986); P. J. Sellers, *ibid.* **6**, 1335 (1985); J. L. Monteith, *Philos. Trans. R. Soc. London Ser. B* **281**, 277 (1977); J. L. Hatfield, G. Asrar, E. T. Kanemasu, *Remote Sensing Environ.* **14**, 65 (1984); C. S. T. Daughtry, K. P. Gallo, M. E. Bauer, *Agron. J.* **75**, 527 (1983); G. Asrar, E. T. Kanemasu, G. P. Miller, R. L. Weiser, *IEEE Trans. Geosci. Remote Sensing* **GE24**, 76 (1986).
22. C. J. Tucker, B. N. Holben, J. H. Elgin, J. E. McMurtrey, *Remote Sensing Environ.* **11**, 171 (1981); G. Asrar, E. T. Kanemasu, R. D. Jackson, P. J. Pinter, *ibid.* **17**, 211 (1985); C. J. Tucker, C. L. Vanpraet, M. J. Sharman, G. Van Ittersum, *ibid.* **17**, 233 (1985); G. Gosse *et al.*, *Agronomie* **6**, 47 (1986); S. D. Prince, *Int. J. Remote Sensing* **12**, 1301 (1991).
23. Precipitation varies from <100 mm year^{-1} in the Sahara Desert to ~400 mm year^{-1} at the southern boundary of the Sahel zone; a precipitation gradient of ~1 mm year^{-1} km^{-1} occurs from ~18°N to ~10°N (*2, 24*). The Sahara Desert, Sahel zone, and their transition zone have been defined as having the following rainfall values: 0 to 100 mm year^{-1}, Sahara Desert; 100 to 200 mm year^{-1}, Saharan-Sahelian transition zone; and 200 to 400 mm year^{-1}, Sahel proper. Rainfall in this area is unimodal and occurs from July to October; the rest of the year is dry (*2, 3, 24, 25*).
24. F. White, *The Vegetation of Africa* (Unesco, Paris, 1983).
25. H. Breman and C. T. de Wit, *Science* **221**, 1341 (1983).
26. Data from NOAA-6 (1980), NOAA-7 (1981 to 1984), NOAA-9 (1985 to 1988), and NOAA-11 (1989 to 1990) were used from 1 July to 31 October of 1980 to 1990. Daily AVHRR 4-km data were acquired for Africa, the NDVI was formed from channel 1 and channel 2 as $(2 - 1)/(2 + 1)$, a cloud mask using channel 5 was applied labeling everything colder than 12°C as cloud, and the data were mapped to an equal-area projection with a ~7.6-km grid cell. The daily mapped data were formed into 10-day images and averaged for each year. Formation of composite images minimizes atmospheric effects, scan angle effects, cloud contamination, and solar zenith angle effects [B. N. Holben, *Int. J. Remote Sensing* **7**, 1417 (1986); M. Shibayama, C. L. Wiegand, A. J. Richardson, *ibid.*, p. 233; K. J. Ranson and C. S. T. Daughtry, *IEEE Trans. Geosci. Remote Sensing* **GE25**, 502 (1987)]. Calibration corrections after Y. J. Kaufman and B. N. Holben (*Int. J. Remote Sensing*, in press) were applied. A total of 4500 orbits of AVHRR data were used.
27. A table with the estimated 200 mm year^{-1} isoline boundary from 15.5°W to 38.5°E at 0.5° longitude increments from 1980 to 1990 is available from the authors upon request.
28. H. N. Le Houerou and C. H. Hoste, *J. Range Manag.* **30**, 181 (1977); M. C. Rutherford, *S. Afr. J. Sci.* **76**, 53 (1980); M. K. Seely, *ibid.* **74**, 295 (1978).
29. We thank D. Rosenfelder, J. Rosenfelder, and R. Rank for assistance.

12 February 1991; accepted 15 May 1991

Organic Molecular Soft Ferromagnetism in a Fullerene C_{60}

PIERRE-MARC ALLEMAND, KISHAN C. KHEMANI, ANDREW KOCH, FRED WUDL, KAROLY HOLCZER, STEVEN DONOVAN, GEORGE GRÜNER, JOE D. THOMPSON

The properties of an organic molecular ferromagnet [$C_{60}TDAE_{0.86}$; TDAE is tetrakis(dimethylamino)ethylene] with a Curie temperature T_c = 16.1 kelvin are described. The ferromagnetic state shows no remanence, and the temperature dependence of the magnetization below T_c does not follow the behavior expected of a conventional ferromagnet. These results are interpreted as a reflection of a three-dimensional system leading to a soft ferromagnet.

THE QUEST FOR A NONPOLYMERIC organic ferromagnet has intensified during the past 5 years with varying results (*1–10*). Curie temperatures (T_c's) on the order of 1 to 2 K have been observed (*7–12*). An organometallic molecular ferromagnet with T_c of ~4 K has been known for sometime (*13*), and similar systems with T_c of 6.2 K (*14*) and 8.8 K (*15*) have recently been reported. Polymeric ferromagnets with T_c's claimed to be greater than 300 K have also been described but their characterization remains incomplete (*2, 16*), and the possibility of a polaronic, polymeric ferromagnet has appeared (*17*). We report on the preparation and preliminary characterization of an organic molecular solid with a transition at 16 K to a soft ferromagnet state.

Our interest in the preparation of materials based on the reduction (*n*-doping) (*18, 19*) of fullerenes (*20–25*) prompted us to explore the use of strong organic reducing agents such as tetrakis(dimethylamino) ethylene (TDAE). Addition of a 20 M excess of the donor to a solution of C_{60} in toluene in a dry box afforded a black microcrystalline precipitate of $C_{60}(TDAE)_{0.86}$ [or $(C_{60})_{1.16}TDAE$] (*26*). The extremely air-sensitive (*27*) solid was washed with toluene and loaded into a capillary tube prepared from a Pasteur pipette, which had been previously sealed at the narrow end. The wide bore end of the pipette was then connected to a 5-mm vacuum stopcock, and the pipette was removed from the dry box to seal the sample under He in a vacuum line at ~2 cm above the powder fill line. The sample was then cooled in zero field in an ac susceptometer and then allowed to warm in an applied field of ≤0.1 Oe. Surprisingly, the transition observed was apparently to a ferromagnetic state.

The sample was studied in greater detail by dc magnetization (M) measurements taken on a Quantum Design superconducting quantum interference device (SQUID) magnetometer. Care was taken to ensure that the sample was not exposed to a field gradient greater than 0.03% of the applied field. In Fig. 1 we show M as a function of T for the sample cooled and warmed in an applied field H_a ~ 1 Oe. Two significant observations can be made from Fig. 1: (i) although M increases sharply below T_c ~ 16.1 K as expected for a ferromagnet, the temperature dependence of M does not follow that of conventional mean field theory; and (ii) within experimental error, there is no hysteresis between cooling and warming. The structure in $M(T)$ below 10 K is field-dependent; similar measurements in applied fields of 10, 100, and 1000 Oe show that with increasing field the minimum at 8 K

P.-M. Allemand, K. C. Khemani, A. Koch, F. Wudl, Departments of Chemistry and Physics and Institute for Polymers and Organic Solids, University of California, Santa Barbara, CA 93106.
K. Holczer, S. Donovan, G. Grüner, Department of Physics, University of California, Los Angeles, CA 90024.
J. D. Thompson, Los Alamos National Laboratory, Los Alamos, NM 87545.